Nucleic Acids Research, 2005, Vol. 33, No. 7 ***2141–2152***
doi:10.1093/nar/gki505

Ribonucleases J1 and J2: two novel endoribonucleases in *B.subtilis* with functional homology to *E.coli* RNase E

Sergine Even, Olivier Pellegrini, Lena Zig, Valerie Labas[1], Joelle Vinh[1], Dominique Bréchemmier-Baey and Harald Putzer*

CNRS UPR9073, IBPC, 13 rue P. et M. Curie, 75005 Paris, France and [1]CNRS UMR7637, ESPCI, 10 rue Vauquelin 75005 Paris, France

Received February 25, 2005; Revised and Accepted March 24, 2005

ABSTRACT

Many prokaryotic organisms lack an equivalent of RNase E, which plays a key role in mRNA degradation in *Escherichia coli*. In this paper, we report the purification and identification by mass spectrometry in *Bacillus subtilis* of two paralogous endoribonucleases, here named RNases J1 and J2, which share functional homologies with RNase E but no sequence similarity. Both enzymes are able to cleave the *B.subtilis thrS* leader at a site that can also be cleaved by *E.coli* RNase E. We have previously shown that cleavage at this site increases the stability of the downstream messenger. Moreover, RNases J1/J2 are sensitive to the 5′ phosphorylation state of the substrate in a site-specific manner. Orthologues of RNases J1/J2, which belong to the metallo-β-lactamase family, are evolutionarily conserved in many prokaryotic organisms, representing a new family of endoribonucleases. RNases J1/J2 appear to be implicated in regulatory processing/maturation of specific mRNAs, such as the T-box family members *thrS* and *thrZ*, but may also contribute to global mRNA degradation.

INTRODUCTION

In the past decade, interest in messenger RNA maturation/degradation in bacteria has increased considerably, since it has been shown to be an important element in the control of gene expression. RNA turnover is not only a powerful tool to permit rapid adaptation to nutritional or environmental changes, but it also enables the cell to efficiently control the stoichiometry of proteins encoded within a single operon (1–5). RNA degradation has mostly been studied in *Escherichia coli*, and has led to the identification and characterization of many endo- and exoribonucleases involved in transcript turnover. According to current knowledge, mRNA degradation in *E.coli* generally initiates with an endonucleolytic cleavage (6–8). This first step is rate-limiting and is mediated mainly by RNase E. This enzyme, which is essential for cell viability, cleaves predominately in AU-rich single-stranded regions (9–11). The activity depends upon the nature of the 5′ end of the target mRNA. Monophosphorylated templates are cleaved more efficiently than triphosphorylated mRNAs while circularized substrates are essentially resistant (12–14). The RNA fragments generated by endonucleolytic cleavages are then attacked by 3′–5′-exonucleases, mainly polynucleotide phosphorylase and RNase II, but also RNase R (15).

While the process of RNA degradation is now well documented in *E.coli*, the major players involved in mRNA processing, degradation and stabilization in *Bacillus subtilis* and other Gram-positive bacteria remain elusive. RNase III and a sugar-nonspecific endoribonuclease have been identified in *B.subtilis* (16–18), but this organism has no homologues of the two essential *E.coli* endoribonucleases, RNase E (*rne*) and oligoribonuclease (*orn*). However, an activity similar to the former probably exists in this organism (19). In addition, an increasing amount of data suggests the existence of an enzyme in *B.subtilis* which is sensitive to the nature or the structure of the mRNA 5′ end as is the case for RNase E (20–24). Clearly, our understanding of mRNA processing/degradation in *B.subtilis* requires the identification of the major ribonucleases involved.

During previous studies on the expression of the *B.subtilis thrS* gene, encoding threonyl-tRNA synthetase, we identified an endonucleolytic cleavage near a conserved sequence called the T-box just upstream of a transcription terminator present in the long untranslated leader mRNA (Figure 1, cleavage 2). *thrS* is a member of the T-box family of genes in Gram-positive

*To whom correspondence should be addressed. Tel: +33 1 58 41 51 27; Fax: +33 1 58 41 50 20; Email: putzer@ibpc.fr

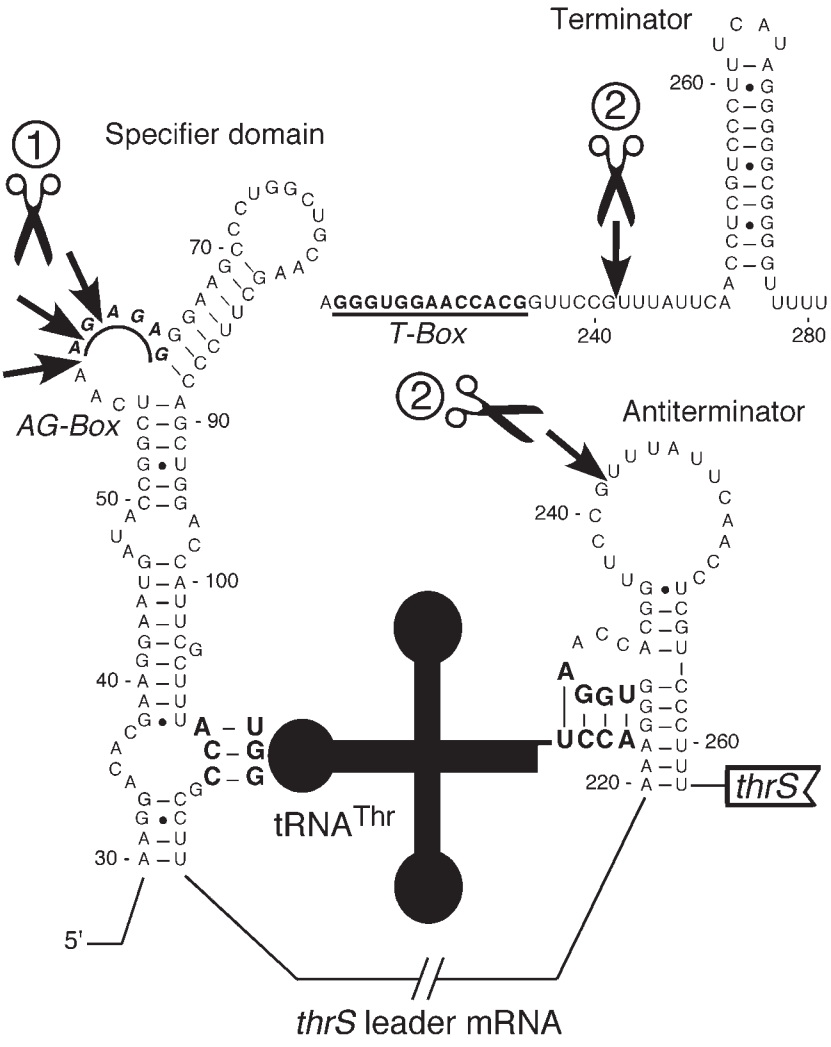

Figure 1. *thrS* mRNA leader: regulation by antitermination and cleavage sites. Under threonine starvation conditions, uncharged $tRNA^{Thr}$ interacts with the *thrS* leader mRNA as illustrated, thereby increasing read-through of the terminator by stabilizing the antiterminator structure. Two RNA cleavage sites are indicated by arrows. Cleavage 1 in the AG-box (see text) was used to trace the novel endoribonuclease activity during purification. Cleavage 2, occurring next to the T-box has previously been shown to stabilize *thrS* read-through transcripts *in vivo* by leaving a stable secondary structure close to the 5′ end of the mRNA (24). *E.coli* RNase E is able to cleave site 2 *in vivo* and *in vitro* (19).

bacteria whose expression is regulated by a tRNA-dependent antitermination mechanism in response to starvation for the cognate amino acid [for a review, see (25)]. Cleavage next to the T-box (Figure 1, cleavage 2) increases the stability of the downstream mRNA probably due to the presence of a stable secondary structure at its 5′ end, i.e. the terminator involved in regulation (24). Cleavage can occur at the same position in *E.coli* where it is RNase E dependent (19). We have identified a second processing site within the specifier domain of the *thrS* leader mRNA (Figure 1, cleavage 1) that can be cleaved *in vitro* by an activity contained in a ribosomal high salt wash (HSW). Here, we describe the purification and identification of two novel endoribonucleases that are responsible for both the cleavages observed in the *thrS* leader. They are also implicated in the processing of the *thrZ* leader encoding a second threonyl-tRNA synthetase in *B.subtilis*. We provide evidence that these two enzymes are paralogues and functionally homologous to *E.coli* RNase E with respect to cleavage specificity and 5′ end dependence.

MATERIALS AND METHODS

Bacterial strains and growth conditions

The prototrophic *Bacillus subtilis* 168 strain 1A2 (BGSC) was used for the purification of RNases J1/J2 and the construction of mutants. In strain SSB340, the *rnjB* (*ymfA*) gene was partially deleted by double-crossover recombination with plasmid pHMJ3. For strain SSB344, the *rnjA* (*ykqC*) gene in strain SSB340 was put under the control of the Pspac promoter by Campbell-type integration of plasmid pHMJ4. Strain SSB30 is derived from the prototrophic strain and carries a deletion of the *thrS* gene constructed by double-crossover recombination with plasmid pHMS15 (26). Strain SSB345 corresponds to strain SSB344 where, in addition, the *thrS* gene has been deleted by transformation with chromosomal DNA of strain SSB30.

E.coli JM 109 served as the host for plasmid constructions. Overexpression of intein fusion proteins was carried out in strain BL21(DE3) (27) carrying plasmid pRARE (Novagen) which overexpresses rare tRNAs.

E.coli was grown at 37°C in LB medium. *B.subtilis* was grown at 37°C in LB or SMS minimal medium (28) supplemented with 0.2% casaminoacids. When required, antibiotics were added at the following concentration: ampicillin (200 μg/ml), tetracyclin (10 μg/ml), neomycin (7 μg/ml), erythromycin (erythromycin and lincomycin at 0.5 and 12.5 μg/ml, respectively).

Plasmid constructions

pHMJ1. The coding sequence of the *rnjA* gene containing an additional C-terminal glycine codon was cloned in phase with the intein domain in plasmid pKYB1 (New England Biolabs) between the sites NdeI and SapI.

pHMJ2. Similar to pHMJ1, but containing the *rnjB* gene with an additional C-terminal glycine codon.

pHMJ3. A 742 bp BmgBI–EcoRI fragment within the *rnjB* gene in plasmid pHMJ2 was replaced with the tetracycline cassette (cleaved with SmaI–EcoRI) of plasmid pDG1515 (29).

pHMJ4. A 407 bp fragment of the *rnjA* gene starting at position −56 with respect to the initiation codon was PCR amplified and ligated as a HindIII–SphI fragment into the respective sites of the integrative plasmid pDG648 (provided by P. Stragier) downstream of the Pspac promoter. Campbell-type integration of pHMJ4 on the *B.subtilis* chromosome renders *rnjA* expression IPTG dependent.

pHMS17. This plasmid contains the promoter, the entire leader sequence and part of the *thrS* structural gene (30).

In vitro transcription

In vitro transcription with *E.coli* (Sigma) or purified *B.subtilis* RNA polymerase (31) was carried out as described in (32) using plasmid pHMS17 linearized by ClaI as template.

In vitro transcription with T7 RNA polymerase was performed as described by the manufacturer (Promega) using PCR fragments as templates. For *thrS* mRNA synthesis, the PCR template was prepared using oligonucleotides HP128 (AGAATTCTAATACGACTCACTATAGGGAGATT AAGAAAGACAC) and HP27 (CCTTGACTGCTCCATCAGGAAATG). It contains the T7 promoter, the entire leader sequence and the first 46 nt of the coding sequence. The *thrZ* template was synthesized with oligonucleotides HP813 (AGAATTCTAATACGACTCACTATAGGGA ATTGAATACATGCGAT) and HP814 (GTCCGGAAGCTGAATGTG). It contains the T7 promoter, part of the leader sequence [downstream of the second leader terminator, position 582 in (26)] and the first 33 nt of the coding sequence. Transcripts were purified by gel filtration on Sephadex G-50 columns. Alternatively, the mRNA substrate was purified from unwanted products by isolation on a 5% polyacrylamide gel.

5′ monophosphorylated ^{32}P-labelled mRNA substrates were synthesized with T7 RNA polymerase as described in (33).

RNase J1/J2 processing assays

The assay mixture (50 μl) contained 20 mM HEPES–KOH (pH 8.0), 8 mM $MgCl_2$, 100 mM NaCl, 0.48 U/μl RNasin (Promega), ^{32}P-labelled mRNA substrate prepared with either *E.coli* or T7 RNA polymerase and a protein fraction. The addition of $MgCl_2$ was necessary to observe cleavage. The reaction was incubated at 30°C for 20 min, stopped by the addition of 5 μl of 3 M Na-acetate pH 5, phenolized and precipitated. The pellet was dissolved in 1× gel loading buffer and run on a denaturing 5% polyacrylamide gel.

Alternatively, assays with purified RNase J1 or J2 proteins were performed in 10 μl of the same reaction mixture. The reaction was stopped by the addition of 5 μl of 3× gel loading buffer and directly loaded on a 5% polyacrylamide gel. The reaction products were visualized on a Phosphorimager and where necessary quantified.

Purification and identification of *B.subtilis* RNases J1 and J2

Endoribonucleolytic activities were isolated from *B.subtilis* ribosomes. All steps were performed at 4°C, and pH of all buffers was adjusted at room temperature. Following growth at 37°C in LB medium supplemented with 0.5% glucose and 20 mM sodium phosphate buffer (pH 7), bacteria were harvested at the end of exponential growth by centrifugation, washed in buffer A (10 mM Tris–HCl, pH 7.5, 15 mM magnesium acetate, 60 mM NH_4Cl and 8 mM β-mercaptoethanol), resuspended in buffer A supplemented with DNase I (10 μg/ml) and disrupted by two passages through a French Press (15 000 psi). After clearing the lysate (27 000 *g*, 30 min), ribosomes were concentrated by ultracentrifugation (190 000 *g*, 1 h 15 min), resuspended in buffer A by gentle agitation, purified by ultracentrifugation through a sucrose cushion (37.7% in buffer A, 165 000 *g*, 17 h) and washed for 2 h under constant stirring with buffer A containing 1 M NH_4Cl. After removal of ribosomes by ultracentrifugation (190 000 *g*, 1 h 15 min), this high salt ribosomal wash was precipitated with 80% ammonium sulfate and dialysed against buffer B (40 mM Bis-Tris, pH 6.5, 4 mM $MgCl_2$, 1 mM DTT and 10% v/v glycerol) containing 50 mM NaCl. The preparation was loaded on a hydroxyapatite column (BioRad). Loosely bound proteins were eliminated by washing the column with 3 M and 50 mM NaCl in buffer B, before applying a 0–1 M K-phosphate, pH 6.8 gradient in buffer containing 4 mM $MgCl_2$, 1 mM DTT and 10% v/v glycerol. Fractions containing the endoribonuclease activity were identified by *in vitro* assays as described above, pooled, dialysed against buffer B containing 50 mM NaCl and fractionated on a Heparin column (Pharmacia) by a 0–2 M NaCl gradient in buffer B. Active fractions were pooled and loaded on a Superdex 200 column (Pharmacia) equilibrated in buffer B containing 150 mM NaCl. Proteins responsible for the endoribonucleolytic activity eluted faster than a 158 kDa marker protein.

Fractions containing the highest activity were analysed on 15% SDS–PAGE and visualized with the SilverQuest Silver staining kit (Invitrogen). For mass spectrometric analysis, the candidate proteins were excised from a Coomassie R-350 stained gel.

Overexpression of RNases J1 and J2 in *E.coli*

Native RNase J1/J2 proteins containing an additional glycine residue at the C-terminal end were isolated using the IMPACT system (New England Biolabs) and following the instructions of the manufacturer. The *rnjA* (*ykqC*) and *rnjB* (*ymfA*) open reading frames were cloned in phase into the intein fusion

vector pKYB1 to give plasmids pHMJ1 and pHMJ2, respectively. Overproduction of fusion proteins was carried out in *E.coli* strain BL21(DE3) containing plasmid pRARE (Novagen).

Mapping of the AG-box processing site

The processing site in the AG-box was mapped by reverse transcription on unlabelled *thrS* leader transcript synthesized *in vitro* with *E.coli* RNA polymerase and processed by HSW as described above. Reverse transcription was performed as described previously (34) using oligonucleotide HP238 (5′-AGTTCCCGTCAGCCATTAC-3′), complementary to positions 151–169 of the *thrS* leader.

Mapping of the processing site upstream of the leader terminator

In order to determine whether the processed fragments contain the 5′ or 3′ ends of the original substrates, the transcripts were ^{32}P-labelled on their 5′ or 3′ ends. For 5′ end-labelling, the nonradioactive mRNA substrates were successively incubated with shrimp alkaline phosphatase (Amersham) and T4 polynucleotide kinase (Biolabs), as described by the manufacturers, using 10 μCi of γ-^{32}P ATP (Amersham). The 3′ end-labelling reaction was performed overnight at 16°C as described in (35) using 50 μCi of ^{32}P pCp (Amersham). The end-labelled transcripts were phenolized, precipitated with ethanol, washed, dried, resuspended in water and subsequently used in 10 μl post-transcriptional processing assays as described above. Sequencing ladders starting at the 5′ or 3′ ends of the mRNA substrates were used for the identification of the cleavage sites.

Measurement of bulk mRNA decay

Total mRNA decay was measured as described previously (36). Briefly, an early-exponential-phase culture was pulse-labelled with [^{3}H]uridine for 2 min; transcription was stopped by the addition of actinomycin D, unlabelled uridine and nalidixic acid. At time intervals from 0 to 10 min, duplicate 1-ml samples were removed and TCA precipitated. Precipitated nucleic acid was collected on Whatman GF/C glass filters. The stable RNA component of radiolabelling was factored out by substracting precipitable counts that remained 60 min after the inhibition of transcription from the counts obtained at all time points.

Database search for RNase J orthologues

At the time of writing 264 prokaryotic genomes (of which the large majority was fully sequenced and annotated) were available on the NCBI Microbial Genomes BLAST database (http://www.ncbi.nlm.nih.gov/sutils/genom_table.cgi) for a protein-based blastp search. Orthologues for RNase J are proposed on the basis of strong overall sequence similarity extending essentially to the entire length of each protein. All alignments were done with *B.subtilis* RNase J1 as well as RNase J2. The results obtained were the same. In addition to overall similarity, we also checked each individual orthologue for the presence of three motifs (motifs A-C, see text) which allow for an assignment of the individual proteins to the β-CASP family of metallo-β-lactamases (37). Potential orthologues of RNase J were only considered as such when the following residues were present: Asp/Glu in motif A, His in motif B and His or a polar amino acid in motif C. Such a configuration has been predicted for members of the β-CASP family involved in RNA metabolism (37).

RESULTS

Identification of an endonucleolytic cleavage in the *thrS* mRNA leader *in vitro*

Cleavage within the so-called specifier domain of *thrS* (Figure 1) was first observed during *in vitro* transcription assays aimed at identifying protein factors promoting tRNA-dependent antitermination. *In vitro* transcription was carried out as described in (32) using purified *B.subtilis* RNA polymerase and linearized plasmid pHMS17 containing the promoter, the entire leader sequence and part of the *thrS* structural gene as template (38). In the presence of a protein fraction isolated from ribosomes (High Salt ribosome Wash), a new signal was generated in addition to the transcript terminated at the leader terminator and the full-length transcript. This signal was also observed in a post-transcriptional assay when incubating a purified *thrS* transcript with HSW or a highly purified fraction containing the processing activity (Figure 2A), indicating this signal was generated by cleavage rather than by transcription arrest. This mRNA was ∼60 nt shorter than the terminated transcript. The processing site was mapped by reverse transcription of the processed *thrS* transcript using an oligonucleotide complementary to positions 151–169 of the *thrS* leader. Cleavage was found to occur at three positions in a single-stranded sequence of the specifier domain. This sequence, known as the AG-box (Figures 1 and 2B), is well conserved in the T-box family of genes and is essential for tRNA-dependent antitermination for reasons not yet known [(39), our unpublished results]. The upstream cleavage product was not detected, probably due to its small size and consequently to its low signal intensity. Moreover, it is likely that this small unprotected RNA is degraded very quickly by exoribonucleolytic activities present in the HSW. Likewise, the signal of the read-through transcript is greatly reduced relative to the 280 nt terminated or 220 nt processed transcript, presumably because it is not protected by secondary structure at the 3′ end.

Two novel endoribonucleases, YkqC and YmfA, are responsible for cleavage of the *thrS* leader mRNA *in vitro*

Further purification of the HSW fraction (by FPLC) was undertaken to isolate the protein(s) responsible for the cleavage observed *in vitro* in the AG-box of the *thrS* leader. The HSW was successively fractionated on hydroxyapatite, heparin and Superdex 200 columns. Throughout the purification, the endoribonucleolytic activity was followed by post-transcriptional cleavage assays as described in Materials and Methods (Figure 2A). The last step, i.e. gel filtration, was found to be crucial for the purification since the active components eluted in fractions corresponding to a high molecular weight component (>158 kDa). In the most active Superdex 200 fraction, we detected only two bands visible on a silver-stained SDS polyacrylamide gel, which was surprising when

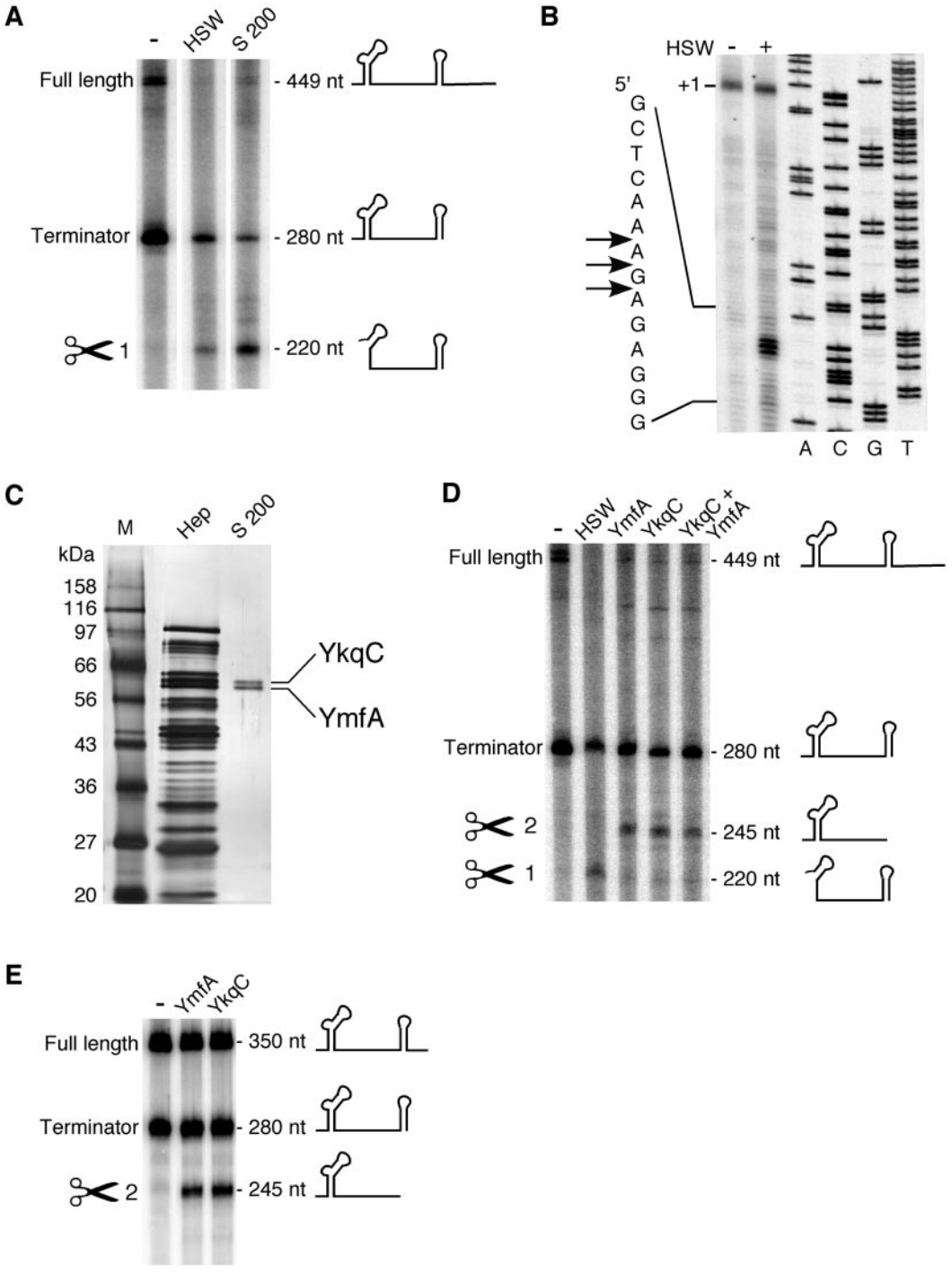

Figure 2. Purification of the nuclease responsible for the cleavage in *thrS* mRNA leader *in vitro*. (**A**) The *thrS* leader was transcribed *in vitro* using plasmid pHMS17 linearized by ClaI as template and *E.coli* RNA polymerase (see Materials and Methods). The *thrS* transcripts, one prematurely terminated at the leader terminator and a read-through transcript, were incubated in 50 µl post-transcriptional assays without the addition of proteins, with 15 µg of a *B.subtilis* ribosomal high salt wash (HSW) or with the most active enriched protein fraction eluting from a Superdex 200 (S 200) column. Scissors indicate the processed transcript. (**B**) Mapping of the processing site shown in (A) in the *thrS* specifier domain. Primer extension was performed with ^{32}P-labelled oligonucleotide HP238 on *thrS* mRNA synthesized *in vitro* in the presence of *B.subtilis* HSW. Arrows indicate the processing sites within the *thrS* specifier domain, referred to as cleavage 1 (Figure 1). A sequencing ladder was run in parallel using the same primer. (**C**) Purification of the endoribonucleolytic activity responsible for cleavage in the *thrS* specifier domain. The most active fractions from the heparin (Hep) and S 200 columns were separated on a 15% SDS–polyacrylamide gel and silver stained. Molecular weight marker proteins (M) were run in the first lane. (**D**) Cleavage of the *thrS* leader transcript by purified YkqC and YmfA proteins. *thrS* mRNA was prepared as described in (A) and incubated in 50 µl post-transcriptional assays without proteins, with 15 µg of a *B.subtilis* HSW or with 200 ng of the purified proteins, YmfA, YkqC and a mixture of YmfA and YkqC. The processed transcripts are indicated by scissors and a number (1: cleavage in the AG-box; 2: cleavage near the T-box, see Figures 1 and 3). (**E**) Cleavage of a *thrS* leader transcript generated with T7 RNA polymerase from a PCR fragment (see Materials and Methods) by purified YkqC and YmfA proteins. The fully synthesized *thrS* mRNA was incubated in 10 µl post-transcriptional assays without any proteins or with 200 ng of the purified proteins, YmfA and YkqC. The processed transcripts are indicated by scissors.

one considers the protein pattern observed after the heparin column (Figure 2C). The molecular weight of the two candidate proteins was estimated to be ~60 kDa, suggesting that the native protein had to be at least a trimer.

The two bands on the SDS polyacrylamide gel were directly analysed by mass spectrometry, which allowed the identification of the two proteins as YkqC (upper band) and YmfA (lower band) both of unknown function (Figure 2C). The two polypeptides contain 555 and 515 amino acids according to the Subtilist webserver (http://genolist.pasteur.fr/SubtiList/). However, a comparison of the proposed YmfA coding sequence with orthologues in other bacteria (see below) and analysis of the putative translation start sites, suggested that the annotation for YmfA was not correct. The true coding sequence appears to start with a TTG codon 120 bp upstream compared to the original annotation, which corresponds to 40 additional amino acids at the N-terminal end. In fact, these additional amino acids can be perfectly aligned with orthologues from related bacteria. This original TTG initiation codon was converted to AUG for overexpression of the protein (see below). Thus, both proteins have the same length and a molecular weight of 61 kDa, which is in good agreement with the observed molecular weights on SDS–PAGE (Figure 2C). In addition, the two proteins are also paralogues sharing 49% identical residues. While YmfA is dispensable, YkqC is considered to be an essential protein (40). From a structural point of view, both proteins belong to the same subgroup of the metallo-β-lactamases, namely the β-CASP family (37), which is thought to be involved in DNA and RNA metabolism (see Figure 6 and Discussion).

The YkqC and YmfA proteins were overexpressed in *E.coli* as intein fusion proteins and purified in a single step after induced self-cleavage of the intein (see Materials and Methods). The purified proteins were then tested in post-transcriptional assays for cleavage of the AG-box in the *thrS* leader. As shown in Figure 2D (cleavage 1), both proteins were able to cleave in the AG-box, but the signal was very weak compared to that observed with the HSW. Unexpectedly, a second cleavage product appeared (Figure 2D, cleavage 2), which had not been observed with the HSW or even the most purified protein fraction from *B.subtilis* (Figure 2A). This fragment of 245 nt was the main cleavage product. The same cleavage pattern was observed when enzymes were used independently or together indicating that YkqC and YmfA possess the same or similar enzymatic activity. Normally the templates for cleavage reactions were prepared using *E.coli* RNA polymerase, but we also used transcripts synthesized by T7 RNA polymerase (see Materials and Methods). The cleavage patterns observed with *E.coli* and T7 RNA polymerase transcripts were quite similar, with the main cleavage product at 245 nt. However, cleavage in the AG-box (cleavage 1), which was very weak on transcripts synthesized by *E.coli* RNA polymerase, was not even detectable with T7 RNA polymerase transcripts.

The second cleavage occurs near the T-box, at the same site previously shown to be an RNase E-dependent cleavage in *E.coli*

In order to identify the site of the second cleavage (Figure 2D and E, cleavage 2), the full-length and terminated *thrS* transcripts synthesized by T7 RNA polymerase were isolated on a polyacrylamide gel and used separately or together in cleavage assays with YkqC and YmfA. Cleavage was observed with both transcripts, generating the same major cleavage product (marked with a scissors symbol in Figure 3A). This fragment thus corresponds to the 5′ part of the *thrS* leader upstream of the cleavage site which is common to the full-length and terminated transcript. This result was confirmed by processing assays on *thrS* leader substrates labelled either at their 5′ or 3′ ends. The major cleavage product was only observed with the 5′ end-labelled transcript (data not shown). A sequencing ladder starting at the 5′ end of the transcript was run in parallel, which allowed us to map the processing site upstream of the *thrS* terminator (around position 243 of the *thrS* leader), in a region corresponding to the loop of the antiterminator (Figure 3A and B). In the case of the full-length transcript, the second fragment originating from this cleavage has a predicted length of ~105 bp corresponding to sequences between the cleavage site and the 3′ end of the transcript. This fragment is present in assays with continuously (Figure 3A, lanes 2, 3, 8 and 9) and 3′ end-labelled (data not shown) transcripts. This result clearly demonstrated that both, YkqC and YmfA, are endoribonucleases. We have previously shown that cleavage at exactly the same position upstream of the *thrS* leader terminator occurs *in vivo* especially under conditions that increase tRNA-mediated antitermination. Processing at this site causes an increase in stability of the downstream mRNA due to the presence of a stable secondary structure (the terminator) close to the 5′ end of the transcript thereby amplifying the effect of antitermination on gene expression (24). When transferred on a plasmid, processing of the *B.subtilis thrS* leader can occur at the same site in *E.coli*, where it is dependent on the endoribonuclease E, both *in vivo* and *in vitro* (19). This suggested that YkqC and YmfA could be functional homologues of *E.coli* RNase E. We decided to rename the two proteins RNase J1 (YkqC) and RNase J2 (YmfA).

RNases J1 and J2 are sensitive to the 5′ phosphorylation state of the mRNA

Considerable data on mRNA decay, mostly from *E.coli*, but also from *B.subtilis* strongly suggest the importance of the 5′ end in the control of mRNA stability (8,12–14,41,42). We therefore analysed the ability of RNases J1 and J2 to 'sense' the 5′ end of the mRNA, by determining the influence of the mRNA 5′ end phosphorylation state on the cleavage rate. Uniformly labelled triphosphorylated and monophosphorylated *thrS* leader transcripts were used as substrates. As shown in Figure 4, the rate of cleavage at site 2 (near the T-box) by RNase J1 (YkqC) was similar with 5′ mono- or triphosphorylated transcripts with a <2-fold increase for the monophosphorylated substrate. Interestingly, we also observed cleavage 1 (in the AG-box), but only for the monophosphorylated transcript (Figure 4A). The two observed cleavages thus have quite different requirements concerning the 5′ phosphorylation state of the transcript. Cleavage in the AG-box clearly depends on a 5′ monophosphorylated RNA whereas cleavage near the T-box is barely affected by the nature of the 5′ end. The results were very similar when replacing RNase J1 by RNase J2 (Figure 4B).

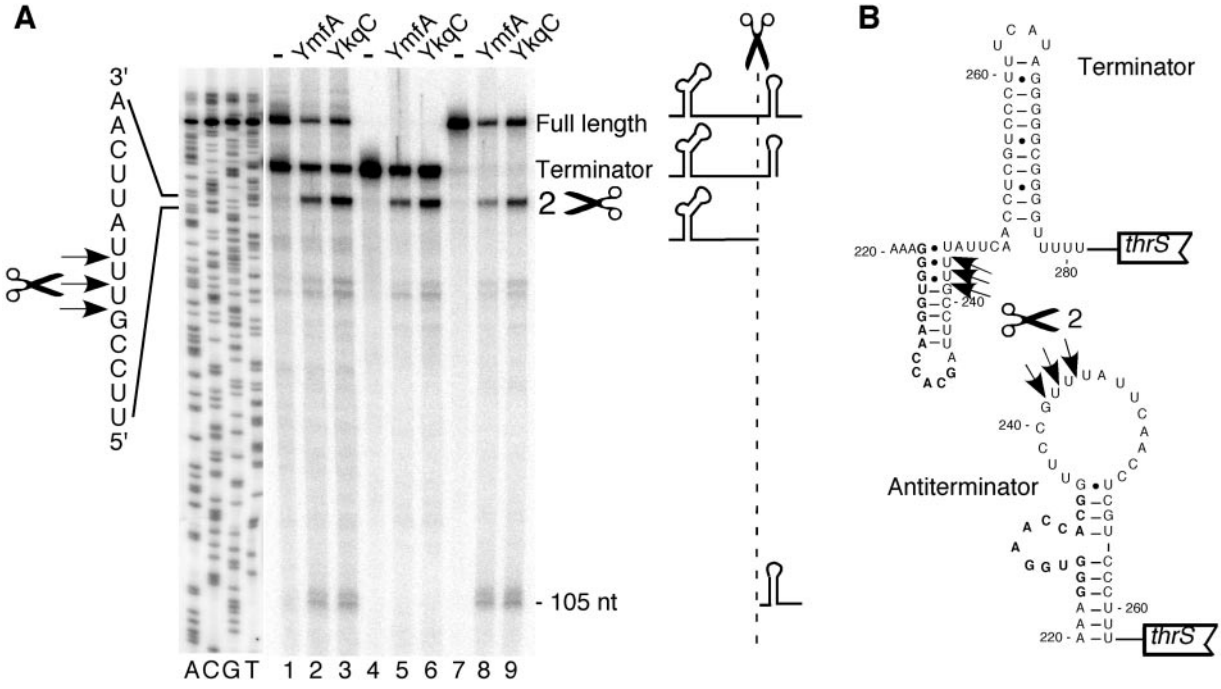

Figure 3. YmfA and YkqC cleave near the T-box. (**A**) *In vitro* transcription was performed as described in Materials and Methods with a PCR fragment corresponding to the *thrS* leader mRNA as template and T7 RNA polymerase. The terminated and full-length transcripts were purified on a 5% polyacrylamide gel and subsequently used together (lanes 1–3) or separately (lanes 4–6 for the terminated transcript and lanes 7–9 for the full-length transcript) in 10 µl post-transcriptional assays. Incubations were performed as described in Materials and Methods without any proteins or with 200 ng of the purified proteins, YmfA and YkqC. The processed transcript is indicated by scissors. A sequencing ladder was run in parallel using primer HP43, which starts at the transcriptional start site of *thrS*. (**B**) T-box processing site in the terminator and antiterminator conformations. T-box is indicated in bold.

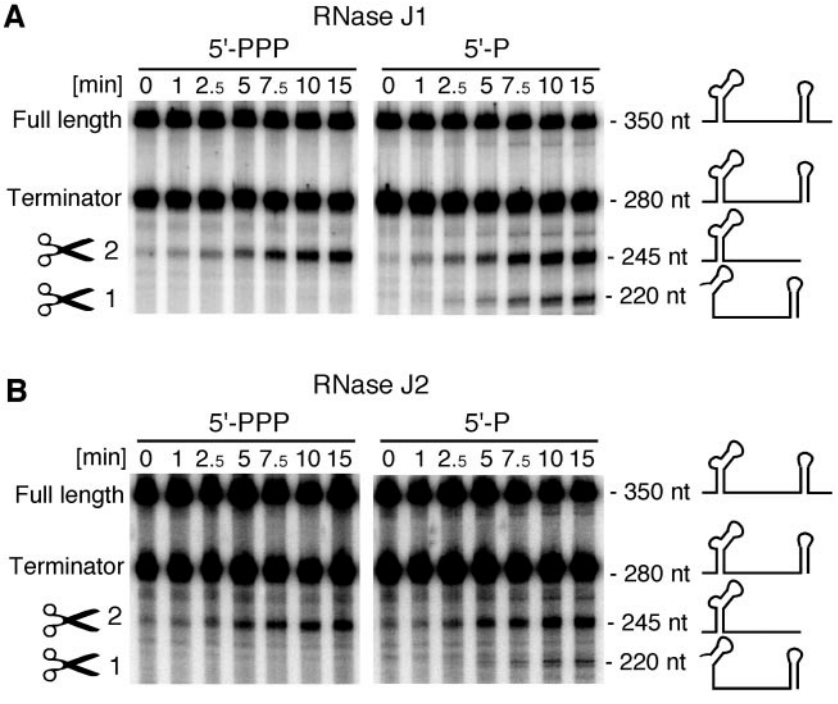

Figure 4. Sensibility of the YkqC (**A**) and YmfA (**B**) processing activity to the 5′ end phosphorylation state of the substrate. Equal amounts of ^{32}P uniformly labelled tri- (lanes 1–7) and monophosphorylated (lanes 8–14) *thrS* leader transcripts were used as substrates in 50 µl post-transcriptional processing assays with 1 µg of YkqC or YmfA. Samples (5 µl) were taken at 0 min (lanes 1 and 8), 1 min (lanes 2 and 9), 2.5 min (lanes 3 and 10), 5 min (lanes 4 and 11), 10 min (lanes 5 and 12), 15 min (lanes 6 and 13) and 20 min (lanes 7 and 14) after addition of purified YkqC (A) or YmfA (B), directly diluted with 2.5 µl of 3× gel loading buffer to stop the reaction and run on a 5% polyacrylamide gel. The processed transcript is indicated by scissors and a number (1: cleavage in the AG-box; scissor 2: cleavage near the T-box).

Cleavage in the AG-box with the Superdex 200 fraction containing a mixture of RNases J1 and J2 was initially observed on a 5′ triphosphorylated transcript (see Figure 2A). However, the initial cleavage rate was 14-fold higher on a 5′ monophosphorylated transcript indicating that the 5′ end dependence of RNases J1/J2 is similar when the proteins are isolated from *B.subtilis* or *E.coli* (data not shown).

RNases J1 and J2 cleave upstream of the terminator in the *thrZ* leader mRNA *in vitro*

In addition to *thrS*, the leader regions of several of the aminoacyl-tRNA synthetase genes of *B.subtilis* regulated by tRNA-dependent antitermination are cleaved *in vivo* between the T-box and the leader terminator (24). We therefore tested the ability of RNases J1 and J2 to cleave a *thrZ* leader transcript *in vitro*. The *thrZ* gene encodes a second threonyl-tRNA synthetase gene, which is normally silent. Its expression is induced in a dose-compensatory manner when expression of the housekeeping *thrS* gene is reduced or the strain is subject to threonine starvation conditions (26). The *thrZ* leader is over 800 bp long and contains three terminators (Figure 5A). Cleavage *in vivo* is observed upstream of the terminator proximal to the structural gene (24). We therefore synthesized a PCR fragment including a T7 promoter covering the *thrZ* leader downstream of the second terminator and the beginning of coding sequence (Figure 5A). As in the case of *thrS*, two transcripts were obtained, a full-length read-through transcript and a shorter one, prematurely terminated at the leader terminator. Both RNases J1 and J2 were able to cleave the *thrZ* transcript *in vitro* (Figure 5B). The processed fragment shown in Figure 5B was also observed with 5′ end-labelled transcripts confirming that it corresponds to the fragment upstream of the cleavage site (data not shown). A sequencing ladder starting at the 5′ end of the transcript was run in parallel, which allowed us to map the processing site near the T-box (Figure 5B), at the same position as previously observed *in vivo* (24).

RNases J1 and/or J2 are required for *thrZ* leader mRNA cleavage *in vivo*

Having shown that RNases J1 and J2 can cleave *in vitro* the 5′ noncoding regions of *thrS* and *thrZ* upstream of the leader terminator, we wanted to verify that these enzymes are also responsible for cleavage *in vivo*. For that purpose, we constructed single and double mutant strains (as described in

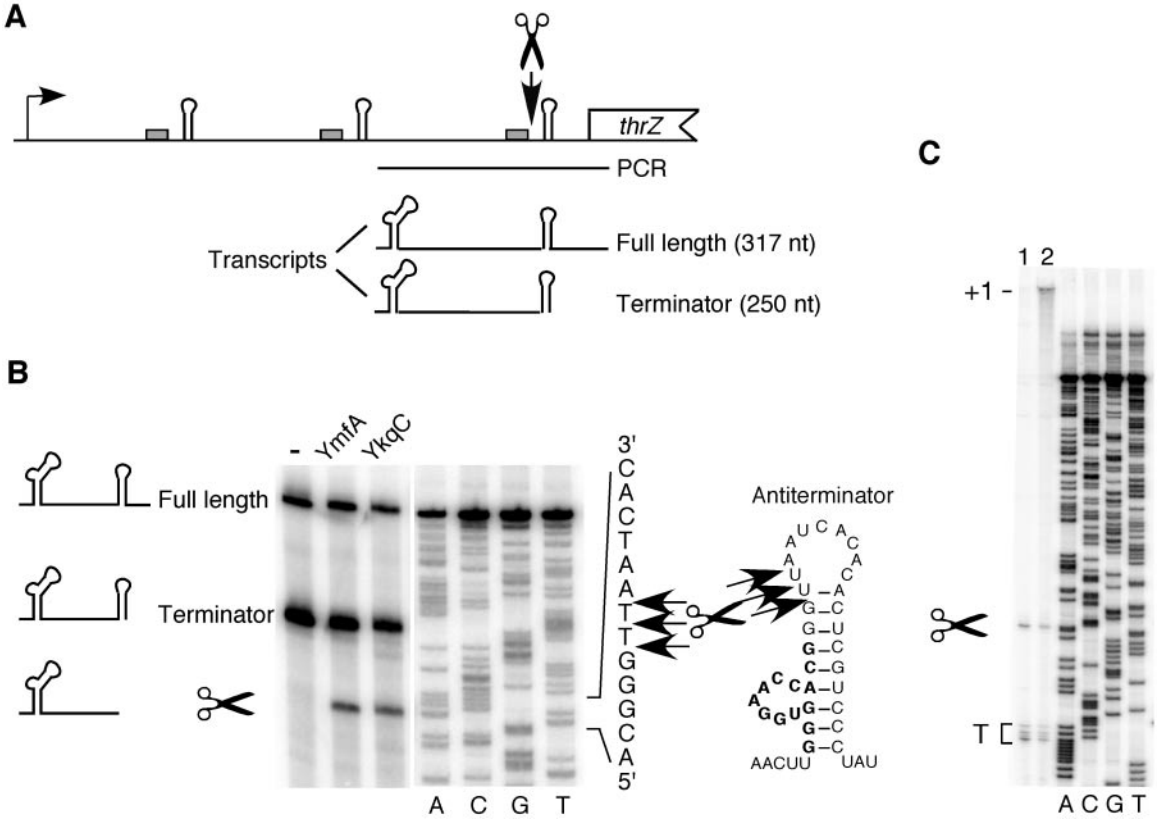

Figure 5. Processing of the *thrZ* mRNA leader *in vitro* and *in vivo*. (**A**) Genetic organization map of the *thrZ* leader. Grey squares indicate the three T-box sequences. The PCR fragment used for *in vitro* transcription (see B) and the transcripts generated are also shown. (**B**) *In vitro* transcription was performed as described in Materials and Methods with T7 RNA polymerase and a PCR fragment corresponding to the *thrZ* leader downstream of the second transcription terminator and the beginning of the coding sequence as template (see A). The two transcripts generated, i.e. the full-length read-through transcript and a shorter one, prematurely terminated at the leader terminator, were incubated in 10 µl post-transcriptional assays without any proteins or with 200 ng of the purified proteins, YmfA and YkqC. The processed transcripts are indicated by a scissors symbol. A sequencing ladder was run in parallel using primer HP 821, which starts at the transcriptional start site of *thrZ* mRNA leader synthesized *in vitro*. Arrows indicate the processing site. T-box is indicated in bold. (**C**) Processing of the *thrZ* mRNA leader *in vivo*. Primer extension was performed with ^{32}P-labelled oligonucleotide HP814 (5′-GTCCGGAAGCTGAATGTG-3′) on total RNA from *B.subtilis* SSB30 (lane 1) and SSB345 (lane 2) as described in Materials and Methods. A sequencing ladder was run in parallel using the same primer. The transcriptional start site of *thrZ* (+1), the processing site near the T-box (scissor) and the non-specific stop at the terminator structure (T) are indicated.

Materials and Methods). In the single mutant, the *ymfA* gene (RNase J2) was partially deleted by a double cross-over event (strain SSB340). For the double mutant, in addition, we put the expression of the chromosomal *ykqC* gene (RNase J1) under the control of the IPTG-inducible Pspac promoter (strain SSB344). A double knock-out strain was not feasible due to the essential nature of the *ykqC* gene. Strain SSB344 grew well in the presence of IPTG in rich and minimal media. In the absence of IPTG, strain SSB344 still grew in LB medium, indicating a certain leakiness of the Pspac promoter. However, in the absence of IPTG, reasonable growth in minimal medium could only be achieved through the addition of casamino acids. This behaviour compromised an *in vivo* analysis of the role of RNases J1 and J2 in the cleavage of the *thrS* leader. Cleavage upstream of the *thrS* terminator *in vivo* is only efficiently detected during threonine starvation, conditions too harsh for the double mutant strain grown in the absence of IPTG.

We therefore turned our efforts to the *thrZ* gene, which is well expressed and whose leader is efficiently cleaved upstream of the third leader terminator in a strain lacking a functional *thrS* gene (24,26). We thus compared the cleavage of *thrZ* transcripts in a *ykqC*, *ymfA* double mutant strain carrying a *thrS* deletion (strain SSB345), grown in the absence of IPTG, and a *thrS* deletion strain, wild-type for the RNase J genes (strain SSB30). Primer extension experiments using an oligonucleotide complementary to positions 16–33 of the *thrZ* coding sequence indicated that the *thrZ* mRNA is efficiently cleaved upstream of the proximal transcription terminator in strain SSB30; practically no signal corresponding to an extension beyond the cleavage site is detectable. In contrast, in strain SSB345 the strongest signal corresponded to position +1, almost 800 nt upstream of the cleavage site (Figure 5C). Thus, reducing the expression of RNase J1 in the total absence of RNase J2 increased the proportion of unprocessed *thrZ* leader (thereby enabling the reverse transcriptase to proceed all the way through to the 5′ end of the *thrZ* transcript). These data strongly suggest that RNase J1 and/or RNase J2 are responsible *in vivo* for the cleavage of the *thrZ* leader mRNA.

Bulk mRNA stability is slightly increased in an RNase J1/J2 double mutant strain

We next investigated whether the presence or absence of the RNase J proteins has an impact on global mRNA stability, as is the case for RNase E in *E.coli*. The decay rate of bulk mRNA was measured by pulse-labelling RNA with ^{3}H-uridine as described in Materials and Methods. Global mRNA half-life was 2.6 ± 0.1 min in a wild-type strain, 2.6 ± 0.3 min in SSB340 (Δ*ymfA*) and 3.6 ± 0.1 min in SSB344 (Δ*ymfA,* Pspac-*ykqC*) when grown in the absence of IPTG. We conclude that the absence of RNase J2 alone has no effect on mRNA stability. However, reducing, in addition, expression of RNase J1 slightly increases global mRNA half-life. This effect is weak but RNase J1 may influence rates of mRNA decay.

DISCUSSION

RNases J1 and J2: functional homologues of *E.coli* RNase E

In this paper, we describe the purification, identification and characterization of two novel endoribonucleases in *B.subtilis*, RNases J1 and J2. In order to be consistent with the current nomenclature, we renamed their genes *rnjA* (*ykqC*) and *rnjB* (*ymfA*). The two *Bacillus* enzymes are, in several aspects, functionally homologous to *E.coli* RNase E.

The most striking similarity is the fact that RNase J1/J2 and RNase E cleave the *thrS* leader at the same position upstream of the terminator. On the other hand, the primary sequence specificity of the *Bacillus* enzymes is apparently low, because there is little primary sequence similarity between the AG-box and the T-box cleavage sites identified in the *thrS* and *thrZ* leaders (Figures 1 and 5). Cleavages occurred rather in single-stranded regions and loops, with structured regions in the vicinity, but without a strong consensus at the sequence level or even a bias toward specific bases as observed for RNaseE.

Another significant correlation between *B.subtilis* RNase J and *E.coli* RNase E, is the sensitivity of cleavage with respect to the 5′ end phosphorylation state of the substrate (12,33). RNases J1 and J2 cleave 5′ monophosphorylated transcripts more rapidly than transcripts with a 5′ triphosphate. Interestingly, the two cleavage sites in the *thrS* leader behave very differently. While the rate of cleavage 2 upstream of the terminator is increased <2-fold on a 5′ monophosphorylated mRNA, cleavage 1 in the AG-box is not even detectable on a 5′ triphosphorylated transcript synthesized by T7 RNA polymerase (Figure 4). This difference suggests that both RNases J1 and J2 may use two different processing/maturation pathways, one being 5′ end dependent, thus sensitive to its phosphorylation state, and the other able to bypass this requirement for efficient cleavage to occur. A similar situation has been described for RNase E. Monophosphorylation of the 5′ end accelerates the reaction, but RNase E seems to also cleave 5′ triphosphorylated transcripts at a basal rate in a 5′ end-independent manner, which is directly related to the intrinsic susceptibility of the site (33). This internal entry pathway with reduced sensitivity to the nature of the 5′ end has been demonstrated by the insertion of 'ectopic' RNase E cleavage sites with high intrinsic susceptibility into an mRNA (43). The *B.subtilis* RNase J cleavage site 2 upstream of the *thrS* leader terminator is thus a good candidate for an equivalent internal entry site. However, in that case, why did we not observe processing at this site in the course of the RNase J purification process from *B.subtilis*? The simplest explanation is based on the fact that even the most purified fraction of RNase J still contained some exoribonucleolytic activity. In contrast to the 220 nt fragment observed by cleavage in the AG-box (Figure 2A), the 245 nt fragment produced by cleavage 2 near the T-box (Figure 2E) lacks a protective secondary structure (the terminator) at its 3′ end. Similarly, the unprotected full-length transcript is also barely detectable under the assay conditions (Figure 2A). However, we will also investigate potential differences in the cleavage specificity of RNase J when isolated from *B.subtilis* or *E.coli*: oligomerization state, existence of heteromultimers in *B.subtilis*, post-translational modifications and presence of a co-factor.

Finally, in a further analogy to RNase E, we measured an increase in global mRNA half-life in a double mutant compared to a wild-type strain (3.6 versus 2.6 min). This effect is small compared to a 2- to 3-fold increase in an *E.coli* RNase E mutant (44), but is nevertheless comparable to that of a null mutant for polynucleotide phosphorylase in *B.subtilis*

(2.8 versus 3.7 min) (36). The latter enzyme plays an important role in mRNA turnover since the primary mode of RNA degradation in *B.subtilis* is phosphorolytic (45). Moreover, in our experiment RNase J1 expression was not abolished but only diminished thereby reducing the potential effect on mRNA stability. However, the small effect of RNase J1/J2 on global mRNA stability might also be due to a smaller set of substrates compared to that of RNase E or to a compensatory effect of stabilizing and destabilizing cleavages. Further investigations will be needed to fully assess the potential importance of this enzyme in mRNA turnover in addition to the more regulatory role established here.

RNases J1 and J2 belong to the β-CASP family of metallo-β-lactamases

From a structural point of view, the paralogous RNases J1 and J2 belong to the β-CASP family of metallo-β-lactamases, which comprise a large number of proteins in all three primary kingdoms, eukaryotes, bacteria and archaea (37). These proteins appear to be specialized towards nucleic acids as suggested by functional data gained for at least one eukaryotic member (46). RNases J1 and J2 are the first prokaryotic proteins of the β-CASP family for which a clear function in RNA metabolism has been demonstrated.

Active members of the metallo-β-lactamase superfamily contain five conserved sequence motifs that participate in zinc coordination and hydrolysis reaction (47,48). The hallmark of the β-CASP subfamily is the presence of three highly conserved amino acids (37) shown as motifs A, B and C in Figure 6. Motif A is an acidic residue (D or E), motif B is always a histidine and motif C confers substrate specificity. This residue is predicted to be a hydrophobic amino acid in enzymes acting on DNA whereas it is always a histidine in RNA-specific proteins. RNase J1, with a Histidine as the C motif, is the first example in prokaryotes that confirms the predictive power of these motifs. The presence of an asparagine in the corresponding position of RNase J2 indicates that motif C can also accommodate a polar amino acid without compromising the endoribonuclease activity (Figure 6).

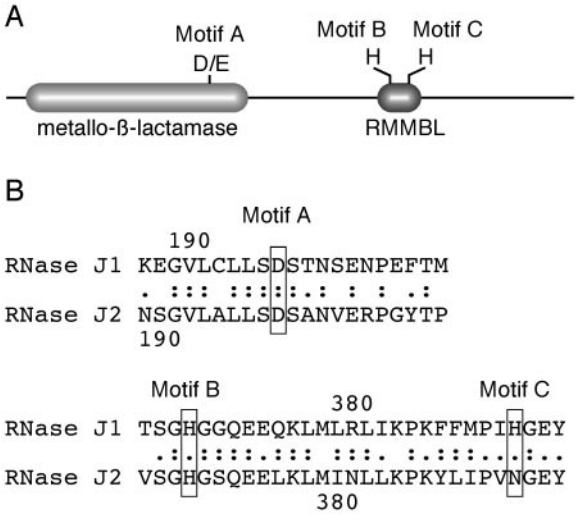

Figure 6. Domain structure of *B.subtilis* RNases J1/J2. (**A**) RNases J1/J2 belong to the β-CASP family recently described by Callebaut *et al*. (37) as a separate group within the metallo-β-lactamase superfamily. These proteins appear to be specialized towards nucleic acids and are characterized by the presence of three highly conserved amino acids, namely motifs A, B and C. Motifs B and C are located in the RNA metabolizing metallo-β-lactamase domain (RMMBL). (**B**) Comparison of motifs A, B and C between RNases J1 and J2.

Orthologues of RNase J1/J2 are widely spread among bacteria and archaea

Clear orthologues of RNase J1/J2 can be found in many bacteria and archaea (see Figure 7). In our search, we considered not only high overall full-length similarity but also checked every individual candidate for the presence of residues D/E in motif A, H in motif B and H or a polar amino acid in motif C. Moreover, all orthologues identified also contain two strictly conserved proline residues between motifs B and C,

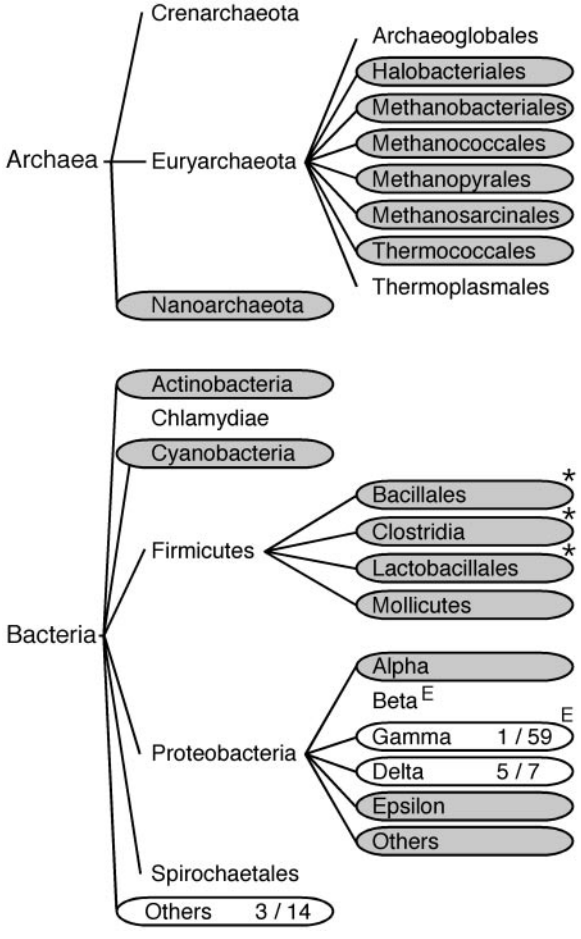

Figure 7. The phylogenetic distribution of RNase J orthologues in prokaryotes. Subfamilies of organisms where at least one member contains an RNase J are encircled. Grey-shaded circles indicate that every single member of this family contains an RNase J orthologue. Ratios refer to the number of members of a subfamily that possess one orthologue to RNase J1/J2 over the total number of members. Subfamilies of the Firmicutes often contain several RNase J orthologues (indicated by an asterisk). Within the *Bacillales* and *Lactobacillales* groups, there is always one orthologue clearly more related to RNase J1 than RNase J2, with the others being equally similar to both. Subfamilies of the *Proteobacteria* containing the classical RNase E and G complement are marked by the letter E.

corresponding to residues 383 and 388 in *B.subtilis* RNase J1 (Figure 6). Most organisms have only a single orthologue, more or less equally similar to RNases J1 and J2 of *B.subtilis* but shorter at the C-terminal end (archaea) or, on the contrary, carrying N-terminal extensions (actinobacteria) or C-terminal extensions (cyanobacteria) compared to the *Bacillus* counterpart. The firmicutes to which *B.subtilis* belongs often have several copies of RNase J orthologues, up to four as in the case of *B.thuringiensis*. Generally, one copy is clearly more related to RNase J1 than RNase J2 with the other copies being equally similar to both *B.subtilis* RNases. It is worth mentioning that the orthologues corresponding to the latter category in the *Lactobacillales* always have a glutamine as motif C equivalent to the asparagine of RNase J2 of *B.subtilis*. Since we have shown that RNase J2 is a functional endoribonuclease, it is likely that these orthologues are also involved in RNA processing. In contrast, the second potential orthologues of *Lactobacillus gasseri/johnsonii* have the hydrophobic amino acid isoleucine as motif C and would thus be predicted to act on DNA rather than RNA (37). The situation is similar in the *Mollicutes* where in all cases a potential second orthologue, despite good overall similarity, does not correspond to the criteria concerning motifs A, B and C.

Finally, there is the case of the proteobacteria, which is interesting because it allows to establish a relationship between the occurrence of RNase E and RNase J. RNase E and RNase G, a close analogue of the catalytic portion of RNase E, always occur together within the β- and γ-subdivisions of the *Proteobacteria*. These two subfamilies do not have an RNase J orthologue, with the unique exception of *Methylococcus capsulatus*. However, a single RNase E/G family member is found in many eubacterial species outside the β- and γ-*Proteobacteria*. In most cases, these enzymes are similar to RNase G in size (∼500 amino acids) and equally similar to both RNase G and the N-terminal half of RNase E. The occurrence of these RNase E/G-like enzymes is not correlated with that of RNase J. For example, *Chlamidiae* have RNase E/G but no RNase J while the *Actinobacteria* have both. A more detailed enzymatical and structural analysis of RNase J and E/G-like proteins is clearly necessary to establish to what extent the functions of RNase E/G and RNase J overlap.

ACKNOWLEDGEMENTS

We wish to thank P. Regnier and J. Plumbridge for useful discussions and critical reading of the manuscript. S.E. benefited from financial support from INRA (ASC). This work was supported by funds from the CNRS (UPR 9073), MRE (Contract 92C0315), Université Paris VII (Contract DRED) and PRFMMIP from the Ministère de l'Education Nationale. Funding to pay the Open Access publication charges for this article was provided by CNRS (UPR 9073).

Conflict of interest statement. None declared.

REFERENCES

1. Drider,D., DiChiara,J.M., Wei,J., Sharp,J.S. and Bechhofer,D.H. (2002) Endonuclease cleavage of messenger RNA in *Bacillus subtilis*. *Mol. Microbiol*., **43**, 1319–1329.
2. Klug,G. and Cohen,S.N. (1990) Combined actions of multiple hairpin loop structures and sites of rate-limiting endonucleolytic cleavage determine differential degradation rates of individual segments within polycistronic puf operon mRNA. *J. Bacteriol*., **172**, 5140–5146.
3. Meinken,C., Blencke,H.M., Ludwig,H. and Stulke,J. (2003) Expression of the glycolytic gapA operon in *Bacillus subtilis*: differential syntheses of proteins encoded by the operon. *Microbiology*, **149**, 751–761.
4. Homuth,G., Mogk,A. and Schumann,W. (1999) Post-transcriptional regulation of the *Bacillus subtilis* dnaK operon. *Mol. Microbiol*., **32**, 1183–1197.
5. Mader,U., Hennig,S., Hecker,M. and Homuth,G. (2004) Transcriptional organization and posttranscriptional regulation of the *Bacillus subtilis* branched-chain amino acid biosynthesis genes. *J. Bacteriol*., **186**, 2240–2252.
6. Coburn,G.A. and Mackie,G.A. (1999) Degradation of mRNA in *Escherichia coli*: an old problem with some new twists. *Prog. Nucleic Acid Res. Mol. Biol*., **62**, 55–108.
7. Grunberg-Manago,M. (1999) Messenger RNA stability and its role in control of gene expression in bacteria and phages. *Annu. Rev. Genet*., **33**, 193–227.
8. Regnier,P. and Arraiano,C.M. (2000) Degradation of mRNA in bacteria: emergence of ubiquitous features. *Bioessays*, **22**, 235–244.
9. Ehretsmann,C., Carpousis,A.J. and Krisch,H.M. (1992) Specificity of *Escherichia coli* endoribonuclease RNAse E: *in vivo* and *in vitro* analysis of mutants in a bacteriophage T4 mRNA processing site. *Genes Dev*., **6**, 149–159.
10. Mackie,G.A. and Genereaux,J.L. (1993) The role of RNA structure in determining RNase E-dependent cleavage sites in the mRNA for ribosomal protein S20 *in vitro*. *J. Mol. Biol*., **234**, 998–1012.
11. McDowall,K.J., Lin-Chao,S. and Cohen,S.N. (1994) A+U content rather than a particular nucleotide order determines the specificity of RNase E cleavage. *J. Biol. Chem*., **269**, 10790–10796.
12. Mackie,G.A. (1998) Ribonuclease E is a 5′-end-dependent endonuclease. *Nature*, **395**, 720–723.
13. Mackie,G.A. (2000) Stabilization of circular rpsT mRNA demonstrates the 5′-end dependence of RNase E action *in vivo*. *J. Biol. Chem*., **275**, 25069–25072.
14. Xu,F. and Cohen,S.N. (1995) RNA degradation in *Escherichia coli* regulated by 3′ adenylation and 5′ phosphorylation. *Nature*, **374**, 180–183.
15. Cheng,Z.F. and Deutscher,M.P. (2005) An important role for RNase R in mRNA decay. *Mol. Cell*, **17**, 313–318.
16. Panganiban,A.T. and Whiteley,H.R. (1983) Purification and properties of a new *Bacillus subtilis* RNA processing enzyme. Cleavage of phage SP82 mRNA and *Bacillus subtilis* precursor rRNA. *J. Biol. Chem*., **258**, 12487–12493.
17. Wang,W. and Bechhofer,D.H. (1997) *Bacillus subtilis* RNase III gene: cloning, function of the gene in *Escherichia coli*, and construction of *Bacillus subtilis* strains with altered rnc loci. *J. Bacteriol*., **179**, 7379–7385.
18. Oussenko,I.A., Sanchez,R. and Bechhofer,D.H. (2004) *Bacillus subtilis* YhcR, a high-molecular-weight, nonspecific endonuclease with a unique domain structure. *J. Bacteriol*., **186**, 5376–5383.
19. Condon,C., Putzer,H., Luo,D. and Grunberg-Manago,M. (1997) Processing of the *Bacillus subtilis* thrS leader mRNA is RNase E-dependent in *Escherichia coli*. *J. Mol. Biol*., **268**, 235–242.
20. Hambraeus,G., Karhumaa,K. and Rutberg,B. (2002) A 5′ stem–loop and ribosome binding site but not translation are important for the stability of *Bacillus subtilis aprE* leader mRNA. *Microbiology*, **148**, 1795–1803.
21. Dreyfus,M. and Joyce,S. (2002) The interplay between translation and mRNA decay in procaryotes. In Lapointe,J. and Brakier-Gingras,L. (eds), *Translational Mechanisms*. Landes Bioscience, Georgetown, TX, pp. 165–183.
22. Agaisse,H. and Lereclus,D. (1996) STAB-SD: a Shine–Dalgarno sequence in the 5′ untranslated region is a determinant of mRNA stability. *Mol. Microbiol*., **20**, 633–643.
23. Sharp,J.S. and Bechhofer,D.H. (2003) Effect of translational signals on mRNA decay in *Bacillus subtilis*. *J. Bacteriol*., **185**, 5372–5379.
24. Condon,C., Putzer,H. and Grunberg-Manago,M. (1996) Processing of the leader mRNA plays a major role in the induction of *thrS* expression following threonine starvation in *B*. subtilis. *Proc. Natl Acad. Sci. USA*, **93**, 6992–6997.
25. Putzer,H. and Laalami,S. (2002) Regulation of the expression of aminoacyl-tRNA synthetases and translational factors. In Lapointe,J. and

Brakier-Gingras,L. (eds), *Translational Mechanisms*. Landes Bioscience, Georgetown, TX, pp. 388–415.
26. Putzer,H., Gendron,N. and Grunberg-Manago,M. (1992) Co-ordinate expression of the two threonyl-tRNA synthetase genes in *Bacillus subtilis*: control by transcriptional antitermination involving a conserved regulatory sequence. *EMBO J.*, **11**, 3117–3127.
27. Studier,F.W. and Moffatt,B.A. (1986) Use of bacteriophage T7 RNA polymerase to direct selective high-level expression of cloned genes. *J. Mol. Biol.*, **189**, 113–130.
28. Spizizen,J. (1958) Transformation of biochemically deficient strains of *Bacillus subtilis* by deoxyribonucleate. *Proc. Natl Acad. Sci. USA*, **44**, 407–408.
29. Guerout-Fleury,A.M., Shazand,K., Frandsen,N. and Stragier,P. (1995) Antibiotic-resistance cassettes for *Bacillus subtilis*. *Gene*, **167**, 335–336.
30. Gendron,N., Putzer,H. and Grunberg-Manago,M. (1994) Expression of both *Bacillus subtilis* threonyl-tRNA synthetase genes is autogenously regulated. *J. Bacteriol.*, **176**, 486–494.
31. Moran,C.P. (1990) Measuring gene expression in *Bacillus*. In Harwood,C.R. and Cutting,S.M. (eds), *Molecular Biological Methods for Bacillus*. John Wiley & Sons Ltd, Chichester, pp. 267–293.
32. Putzer,H., Condon,C., Brechemier-Baey,D., Brito,R. and Grunberg-Manago,M. (2002) Transfer RNA-mediated antitermination *in vitro*. *Nucleic Acids Res.*, **30**, 3026–3033.
33. Jiang,X., Diwa,A. and Belasco,J.G. (2000) Regions of RNase E important for 5′-end-dependent RNA cleavage and autoregulated synthesis. *J. Bacteriol.*, **182**, 2468–2475.
34. Uzan,M., Favre,R. and Brody,N.E. (1988) A nuclease that cuts specifically in the ribosome binding site of some T4 mRNAs. *Proc. Natl Acad. Sci. USA*, **85**, 8895–8899.
35. Li,Z., Pandit,S. and Deutscher,M.P. (1998) Polyadenylation of stable RNA precursors *in vivo*. *Proc. Natl Acad. Sci. USA*, **95**, 12158–12162.
36. Wang,W. and Bechhofer,D.H. (1996) Properties of a *Bacillus subtilis* polynucleotide phosphorylase deletion strain. *J. Bacteriol.*, **178**, 2375–2382.
37. Callebaut,I., Moshous,D., Mornon,J.P. and de Villartay,J.P. (2002) Metallo-beta-lactamase fold within nucleic acids processing enzymes: the beta-CASP family. *Nucleic Acids Res.*, **30**, 3592–3601.
38. Putzer,H., Laalami,S., Brakhage,A.A., Condon,C. and Grunberg-Manago,M. (1995) Aminoacyl-tRNA synthetase gene regulation in *Bacillus subtilis*: induction, repression and growth-rate regulation. *Mol. Microbiol.*, **16**, 709–718.
39. Rollins,S.M., Grundy,F.J. and Henkin,T.M. (1997) Analysis of cis-acting sequence and structural elements required for antitermination of the *Bacillus subtilis* tyrS gene. *Mol. Microbiol.*, **25**, 411–421.
40. Kobayashi,K., Ehrlich,S.D., Albertini,A., Amati,G., Andersen,K.K., Arnaud,M., Asai,K., Ashikaga,S., Aymerich,S., Bessieres,P. *et al.* (2003) Essential *Bacillus subtilis* genes. *Proc. Natl Acad. Sci. USA*, **100**, 4678–4683.
41. Bechhofer,D.H. (1993) 5′ mRNA stabilisers. In Belasco,J.G. and Brawerman,G. (eds), *Control of Messenger RNA Stability*. Academic Press, San Diego, pp. 31–52.
42. Emory,S.A., Bouvet,P. and Belasco,J.G. (1992) A 5′-terminal stem-loop structure can stabilize mRNA in Escherichia coli. *Genes Dev.*, **6**, 135–148.
43. Baker,K.E. and Mackie,G.A. (2003) Ectopic RNase E sites promote bypass of 5′-end-dependent mRNA decay in *Escherichia coli*. *Mol. Microbiol.*, **47**, 75–88.
44. Babitzke,P. and Kushner,S.R. (1991) The Ams (altered mRNA stability) protein and ribonuclease E are encoded by the same structural gene of *Escherichia coli*. *Proc. Natl Acad. Sci. USA*, **88**, 1–5.
45. Deutscher,M.P. and Reuven,N.B. (1991) Enzymatic basis for hydrolytic versus phosphorolytic mRNA degradation in *Escherichia coli* and *Bacillus subtilis*. *Proc. Natl Acad. Sci. USA*, **88**, 3277–3280.
46. Ryan,K., Calvo,O. and Manley,J.L. (2004) Evidence that polyadenylation factor CPSF-73 is the mRNA 3′ processing endonuclease. *RNA*, **10**, 565–573.
47. Daiyasu,H., Osaka,K., Ishino,Y. and Toh,H. (2001) Expansion of the zinc metallo-hydrolase family of the beta-lactamase fold. *FEBS Lett.*, **503**, 1–6.
48. Aravind,L. (1999) An evolutionary classification of the metallo-beta-lactamase fold proteins. *In Silico Biol.*, **1**, 69–91.